Influence of corrosion rates on polarization and current distribution of ICCP in concrete

Shamir Bhuiyan* and *David* Law[1]

[1]RMIT University, Melbourne, VIC, 3001, Australia

Abstract. Corrosion rate is known to be a factor affecting the distribution of current in cathodic protection (CP) applications. This paper demonstrates the effect of different corrosion rates of embedded steel in concrete on the polarization and distribution of current during CP application. A concrete specimen was cast with separate steel bars at a fixed distance from a centralised anode. The bars are embedded in sections containing different admixed chloride concentrations to create varying corrosion rates. The specimen was conditioned to allow development of corrosion followed by application of short-term CP at a constant current of 20mA/m^2. The magnitude of current flowing to each section was logged along with corresponding potential shifts. Trends were then correlated to the corrosion rates together with circuit resistance. Circuit resistance was shown to predominantly control current distribution whereas corrosion rates had a significant influence on polarization.

1 Introduction

The non-uniform nature of current distribution creates a challenge in the design of an impressed current cathodic protection system to protect the total area of steel reinforcement adequately, whilst avoiding overprotection of any areas. The behaviour of current distribution can be difficult to predict as it is influenced by several different factors occurring simultaneously. This can include applied current density, concrete resistance, reinforcement geometry/arrangement and corrosion rates [1-4].

The presence of actively corroding steel in concrete has been shown to make the distribution of current during cathodic protection uneven, favouring bars closest to the anode, provided corrosion rates do not vary between the bars [1-3]. This distortion appears to increase with corrosion activity [5]. Current distribution can be further complicated in the presence of an active-passive couple [6,7]. Studies have shown that bars with higher corrosion rates require a greater amount of cathodic current to overcome the corrosion. Predictions using computer and theoretical models [2,7] show that current requirements can increase several times over in order to provide the same level of polarization for a corroding bar in contrast to a passive bar. The throwing power is shown to be significantly affected by corrosion rates in galvanic CP, with a higher corrosion rate resulting in a lower throwing power [3,8].

While it is commonly thought that current tends to flow to anodic areas due to lower polarization resistance, it has been found that this may not be the case where a galvanic couple exists [9]. This is further supported by studies [7,10] which showed that in the case of an active-passive couple, cathodic current tends to preferentially flow to passive bars even when geometry and resistivity may favour active bars, until the current is increased to the point where the macrocell current is overcome.

To further the understanding of current distribution, this paper studies the effect of corrosion rates on current distribution and polarization during the application of CP. As concrete resistivity is known to play a large role in current distribution, the study was designed to minimise this effect by maintaining equidistance between the anode and bars, however slight differences in resistivity are expected due to the different chloride concentrations used in the concrete. Given that it is not possible to quantify current flowing to each section of a continuous bar, separate bars were cast in each section to simulate the corresponding areas of the continuous bar. Potentials for the separate and continuous bars are compared.

2 Methodology

A concrete block measuring 300x300x85mm having 3 equal parts separated by acrylic sheets was cast, with 0, 2.5 and 5% NaCl by weight of cement, as shown in Fig1. A MMO titanium ribbon anode strip was placed in the centre and spanned the length of the specimen. The cover varied between 1-5mm due to the wavy nature of the anode (usually packed in rolls). On one side of the anode, three 85mm steel bars were placed in each of the sections while on the opposite side, a single 315mm continuous bar spanned the length of the specimen, going through each section. All bars had a nominal diameter of 12mm and a concrete cover of 35mm (from the base). Lengths of PVC tubing plugged with porous wooden stoppers were used to create housings for Cu/$CuSO_4$ reference electrodes. These were positioned directly above each bar. References were embedded and positioned in the mid

* Corresponding author: Eng.sbhuiyan@outlook.com

span of each section, as shown in Fig 1. Prior to testing, each tube was filled with $CuSO_4$ solution and a copper wire was immersed to create the reference cell.

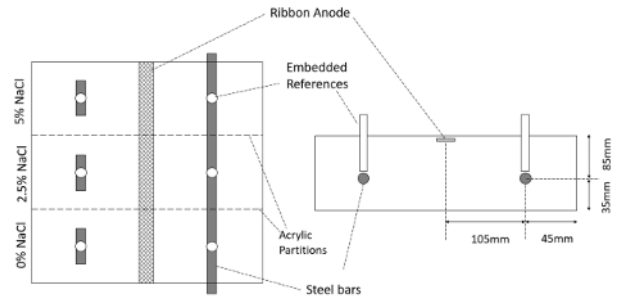

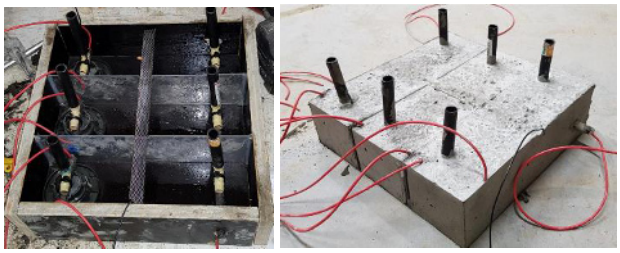

Fig 1 : Specimen arrangement

The concrete mix used was a standard 40MPa concrete mix, the details of which are provided in **Table 1**. Specimens were cast in a single mix Initially a 0% chloride mix which was placed in two layers and vibrated for 30 seconds. Chloride was added to mix to make a 2.5 % chloride content and placed as per the 9% mix, followed by adding further chloride to the mix to make the 5% chloride concrete. The procedure was designed to ensure a single mix was used minimising time between placement and to minimise the risk of crevice corrosion.

Table 1: Mix design

Constituent	Quantity (kg/m^3)
Cement (GP)	391
Water (w/c: 0.65)	253
Fine Aggregate	585
Coarse Aggregate (7mm)	586
Coarse Aggregate (10mm)	586

The test presented in this paper was conducted following more than 3 years since the date of casting, during which the specimen sat in storage following tests from a previous experiment. Prior to testing, the specimen was subject to cyclic spraying in a spray cabinet for one month to promote corrosion of the steel bars. Corrosion rates of each of the separate bars were derived using the LPR (linear polarization resistance) method, utilising the ribbon anode as the auxiliary electrode and corresponding embedded references in each section to measure the polarization of the bars. Following corrosion rate measurements, the sample was allowed to stabilize after which a galvanostatic cathodic polarization test was performed. A constant current of 20mA/m^2 (of total steel area in the specimen) was applied using a galvanostat (ACM Field Machine) and the current flowing to each bar was calculated by logging the voltage drop across fixed resistors (120Ω) connected in series to each circuit and converted using Ohm's law. Moreover, potentials were also logged for each bar. A simplified wiring schematic of the setup is illustrated in Fig 2.

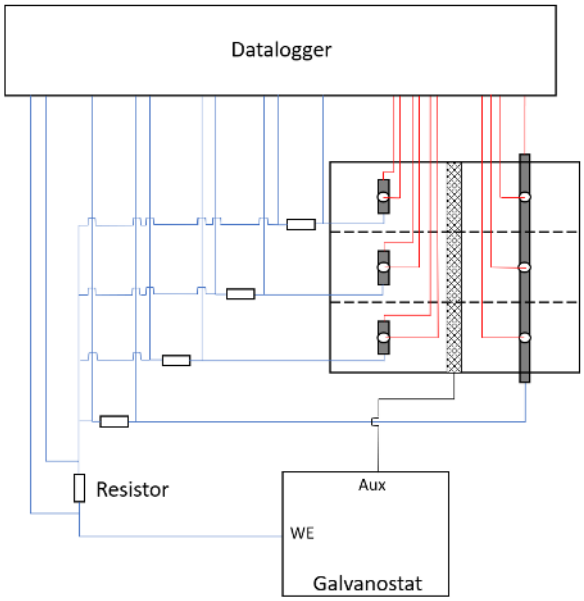

Fig 2: Simplified wiring schematic of test setup

Logging of the data was performed using 2 dataloggers (Datataker DT80/DT85) at a sampling rate of 1 reading every 2 seconds.

3 Results

3.1 Corrosion Rates

Corrosion rates measured are summarised in Fig 3. The general trend observed is as expected, where corrosion rates increase with percentage of admixed salt. The separate bars display larger variation between the bars, with the bar in the 0% NaCl section (designated as '0S') having a corrosion rate two orders of magnitude less than the bars in the 2.5% NaCl section (2.5S) and 5% NaCl section (5S). 0S having a corrosion rate less than 0.1µA/cm^2, indicates that the bar is in a passive state whereas bars 2.5S and 5S have a corrosion rate greater than 1µA/cm^2, which is considered a high level of corrosion [11]. The continuous bar had similar corrosion rates to the separate bars in the 2.5% and 5% zones, corresponding to the sections with active corrosion. However, in the zone corresponding to the 0 % NaCl, the corrosion rate measured on the continuous bar was significantly higher than that for the separate passive bar. This is possibly due to the effect of polarisation on the adjacent active sections of the bars during the corrosion rate measurements. Other possibilities are contamination of the 0% mix by chloride from the 2.5% mix during placement, or crevice corrosion at the junction between the two mixes, though the procedure Adopted was selected to minimise the ;likelihood.

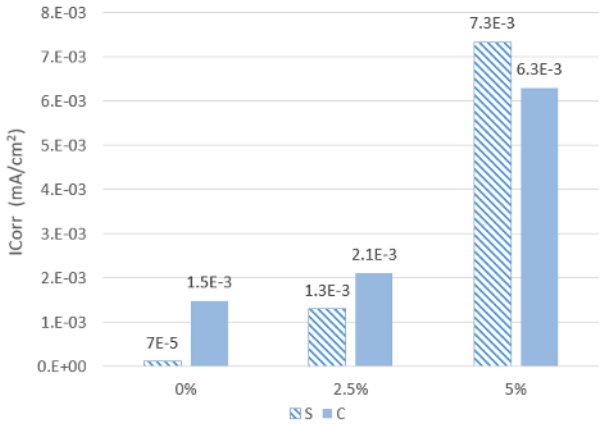

Fig 3: Variation of corrosion rates

3.2 Current distribution

Current distribution was studied by conducting an initial short-term application of current lasting 6 mins. Future studies will investigate the effect of application duration on current and resistance. Fig 4 shows the variation of current during the test period. It was observed at the beginning of the test prior to applying any current that small current values (0±0.02mA) were recorded in each circuit. This is likely due to small macrocell current flowing when the bars are commoned (active-passive couple) as a single connection to the working electrode. These initial values were used to offset the data for the corresponding bars such that initial readings were set to zero. The variation of current between each bar is shown in Fig 4.

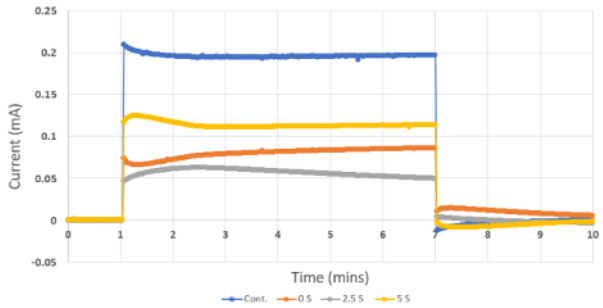

Fig 4: Current distribution to each bar

When current is switched on, different initial trends are observed as changes in interfacial resistance of each bar takes place. This is a function of the polarization resistance and charging of the double-layer capacitance at the steel-concrete interface, the product of which is defined in literature as the *time constant*. It is observed that the separate active bars (2.5S and 5S) display a similar trend with an initial rise in current, whereas the passive bar 0S displays a reduction in the initial current. This reflects the differing time constants between active and passive bars. The continuous bar also behaves differently as it reflects effects from the various sections. The total applied current was logged, (not shown in Fig 4 to avoid distorting the scale of the graph). Data for the total applied current shows a negative current whose magnitude corresponds to the sum of all current flowing to the separate bars at a given point in time.

During the current application, the current received is observed to vary between bars. Fig 5 shows the average current during the on-period for each bar, alongside their corresponding average current densities (= avg.current/bar area).

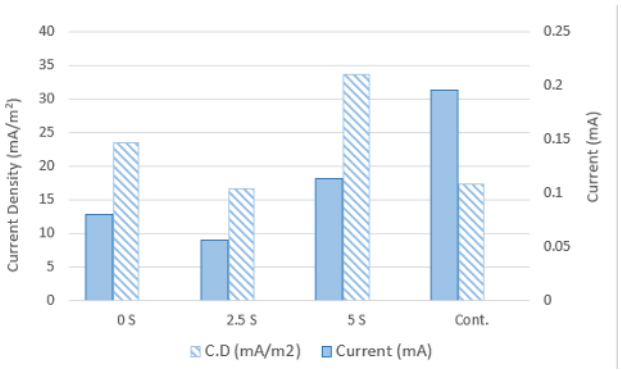

Fig 5: Average current and current densities

While the current applied was calculated to correspond to a current density of 20mA/m^2, it can be seen that the current density at each bar varied significantly, with the highest (5S) requiring 34mA/m^2 and lowest (2.5S) 17mA/m^2. As would be expected, the current density for the separate bars follows the same trend as that of the current received, as the areas of the individual bars are the same. However, the trend for the continuous bar differs and is seen to take the highest current. This can be attributed to the continuous bar having the largest surface area. The larger surface area however results in a lower average current density. Based on the data from the separate bars, it is reasonable to assume the current density for the continuous bar would vary along its length in a similar manner to those of the separate bars. It was observed that bar 0S had a higher current than 2.5S however bar 5S took the most current and had the highest corrosion rate. In order to understand this phenomenon, an *instant-on* current was measured on a separate occasion, to determine circuit resistance for each bar. A 6V DC constant power source was momentarily connected between the anode and each bar sequentially and the initial currents (within 1s of connecting) were recorded using a precision multimeter connected in series and the resistance calculated for each circuit. The initial values are related to the solution resistance of concrete and are thought to be minimally affected by polarization or capacitive effects. The data of the derived circuit resistance is summarised in Fig 6. It is observed that the current data is in line with the circuit resistance data with current and circuit resistance having an inverse relation. Therefore, a consistent trend between current and circuit resistance is observed, while no clear trend between current and corrosion rate is seen. This suggests that the effect of the concrete resistance on current distribution is considerably more prominent than that of corrosion rate and as a result the effects of corrosion rate is unclear. It is expected that the resistance of the chloride contaminated concrete will be lower with increasing concentration of

salt, however an anomaly was observed where 2.5S had a greater resistance than that of 0S. The reason for this is not known, however it may be due to slight differences in bar/anode placement resulting in a more resistive (longer) path for current for 2.5S. Visual inspection of the specimen revealed that the anode had a visibly lower cover in the 2.5% section which perhaps explains the observation.

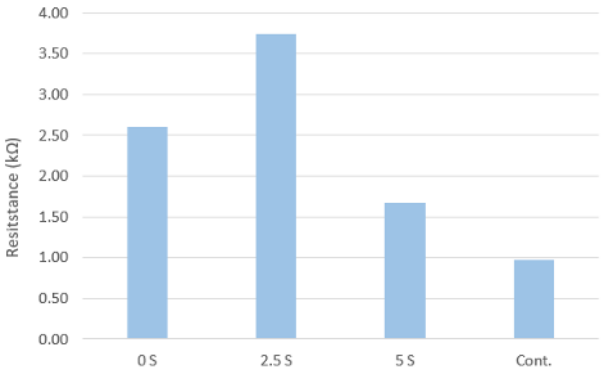

Fig 6: Circuit resistance for each bar

3.3 Polarization

The data logged for steel potentials during the experiment is plotted in Fig 7. The initial potentials are in line with the corrosion rate data, where more negative potentials are seen for bars with higher corrosion rates. The 0C specimen showed a more negative base potential of -416 mV than 0S which had a potential of -367 mV. Once again, it appears that the 0C section of the continuous bar is affected by its adjacent corroding section. During the current-on period, all potentials shifted cathodically however some fluctuations were observed, especially for the 0% specimens. The reason for this is not understood.

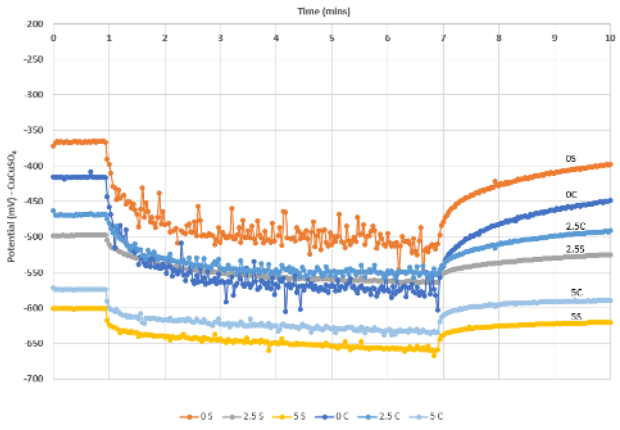

Fig 7: Potential variation during test

Fig 8 shows the polarization calculated for each of the bar sections. Polarization was calculated as the difference between the base potential and instant-off measurement. The data shows that the continuous bar had similar levels of polarization to the separate bars, although slightly higher. This is likely to be due to the larger surface area and therefore receiving higher current than its separate counterparts. Nevertheless, this suggests that the current data measured for the separate bars can be used to approximate the current distribution for each of the sections in the continuous bar, assuming corrosion rates are the same (within each section). It is seen that despite 5S receiving higher current than 0S and 2.5S, it was polarized the least. This is in line with literature, where steel with a higher corrosion rate requires significantly more current to polarize than a bar that is passive.

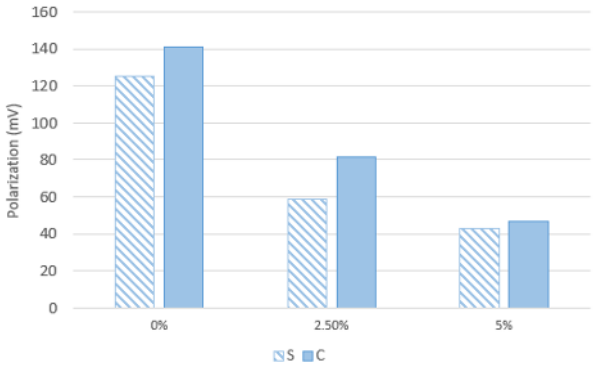

Fig 8: Comparison of polarization data

4 Conclusions

The study presented in this paper demonstrated that circuit resistance had a more prominent effect on current distribution than corrosion rate. Concrete resistance appears to be the governing factor determining current distribution. While polarization is linked to the quantity of current received, the corrosion rate has been shown to be the controlling factor on polarization. This is consistent with literature which shows that an actively corroding bar requires significantly more current to provide the same level of polarization than a passive bar. Further investigation is required to validate the reason for variation of resistivity data and fluctuations observed for potential of passive bars. The study presented in this paper forms a precursor to longer term testing to understand how the current distribution and polarization changes under longer term CP application. Future studies will include application of CP from 6 hours to 1 week and 1 month and will also monitor concrete resistance in comparative control specimens.

Acknowledgements

The authors would like to thank Dr Kate Nairn for her valuable input into the discussion of results in this study.

References

1. A.M. Hassanein, G.K. Glass, N.R. Buenfeld, "Protection current distribution in reinforced concrete cathodic protection systems", *Cement & Concrete Composites* 24, 159–167 (2002)

2. L. Bertolini et al, "Cathodic protection of new and old reinforced concrete structures", *Corrosion Scienc*e 35, 1633-1639 (1993)

3. E. Redaelli, F. Lollini, L. Bertolini, Throwing power of localised anodes for the cathodic protection of slender carbonated concrete elements in atmospheric conditions, *Construction and Building Materials*. 39, 95–104 (2013)

4. J. Xu, W. Yao, "Current distribution in reinforced concrete cathodic protection system with conductive mortar overlay anode", *Construction and Building Materials* 23, 2220–2226 (2009)

5. S. Bhuiyan et al, The effects of anode distance and corrosion activity on current distribution for ICCP systems, MATEC Web of Conferences - Concrete Solutions, 289, Article 03001 (2019)

6. A.A. Sagüés, S.C. Kranc, "On the determination of polarisation diagrams of reinforcing steel in concrete", *Corrosion Science* 48(8), 624–33 (1992)

7. G.K. Glass, A.M. Hassanein, "Surprisingly Effective Cathodic Protection", *Journal of Corrosion Science and Engineering* 4, paper7 (2006)

8. B.V. Belleghem, M. Maes, T. Soetens, Throwing power and service life of galvanic cathodic protection with embedded discrete anodes for steel reinforcement in chloride contaminated concrete, *Construction and Building Materials*, 310, (2021)

9. U. Angst, M. Büchler, On the applicability of the Stern–Geary relationship to determine instantaneous corrosion rates in macro-cell corrosion. *Materials and Corrosion*, 66, 1017-1028, (2015)

10. M.S. Cheung, C. Cao, Application of cathodic protection for controlling macrocell corrosion in chloride contaminated RC structures, *Construction and Building Materials,* 45, 199-207 (2013)

11. C. Andrade, C. Alonso, Corrosion rate monitoring in the laboratory and on-site, *Construction and Building Materials*, 10(5), 315-328 (1996)